Section 1
LASER SYSTEM REPORT

1.A GDL Facility Report

GDL continued operations as a 0.35μm irradiation facility during the first quarter of FY82.

A total of 670 shots were delivered by the facility in the November 1 to December 31, 1981 period. The shot distribution was as follows:

3ω Target Experiments	208	Shots
X-Ray Program	95	
Damage Test Facility	301	
Alignment	66	
TOTAL	670	Shots

During this period the first series of experiments with a 1nsec pulse-width was conducted. Initial measurements included stimulated Raman scattering and continuum x-ray spectroscopy. During this quarter the first series of experiments on kinetic x-ray diffraction was successfully completed and will be discussed in a future issue of the LLE Review.

1.B OMEGA Facility Report

Most of the final quarter of 1981 was spent installing a new one-nanosecond active-passive mode-locked oscillator in the OMEGA driver line.

The new oscillator required an additional optical table, oscillator PFN reconfiguration, and numerous cable and timing changes associated with its longer cavity round trip time of 18.3 nanoseconds (compared to 10.0 nanoseconds for the short-pulse cavity). The beam waist is different as well; this required that we adjust the fill factor with hard aperture and air spatial filter pinhole changes.

Anticipating the driver line restaging that will have to be carried out when the Kuizenga oscillator is incorporated into the OMEGA driver in 1982, we made detailed measurements of the whole-beam energy and near-field beam profile at all significant driver locations. These were used to normalize the energy code, RAINBOW, and to identify any component degradation since the last series of measurements.

With respect to degradation we found that there was very little, if any, permanent change in the driver gains and losses. Realignment of several of the dielectric polarizers in the Pockels cell and Faraday rotator assemblies restored the initially low driver output to design level.

Figure 1 shows the key measurement positions, and Table 1 tabulates the energies measured at these points.

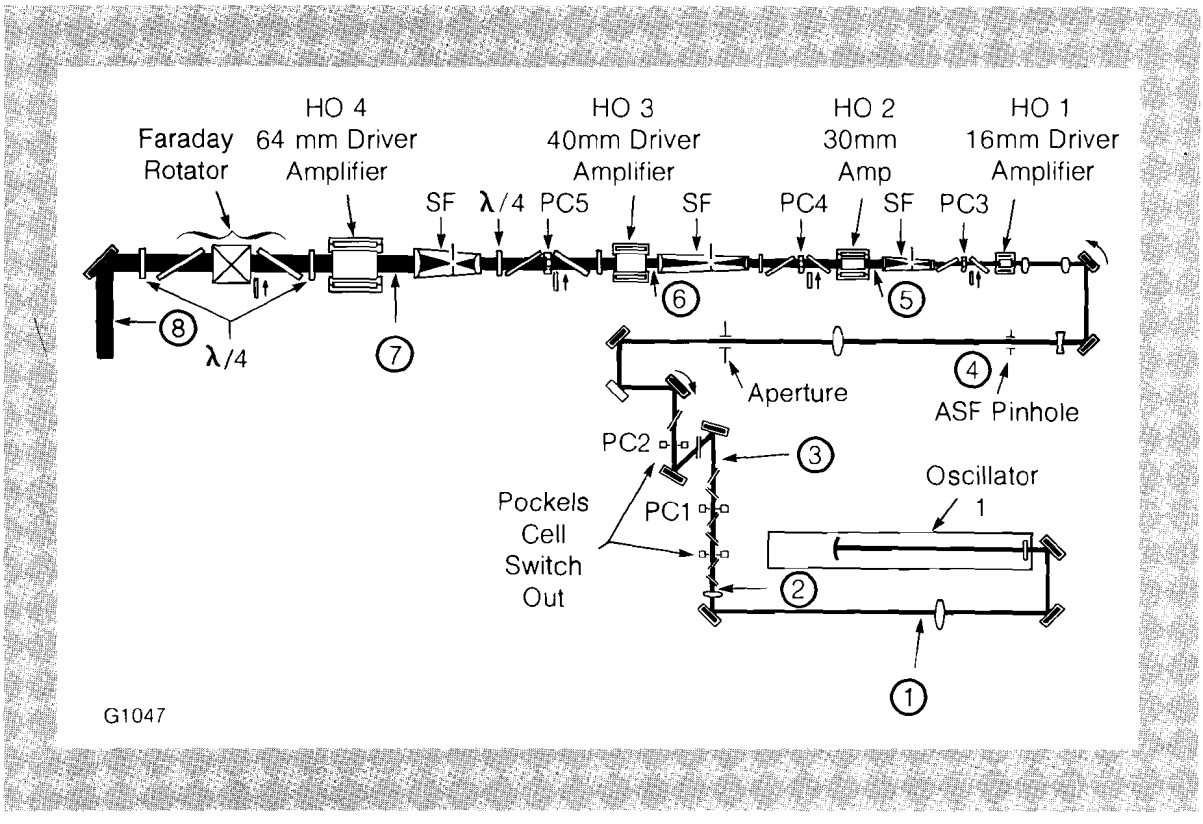

Fig. 1
Staging configuration in the OMEGA driver line. Numbers 1 through 8 indicate positions where beam energy at maximum output was measured for 1 nsec oscillator pulses.

Key	Calorimeter Location	Unamplified Train Energy, μJ	Unamplified Single-Pulse Energy, μJ	Amplified Single-Pulse Energy, J
1	After Collimating Lens	10,000	~500 (est.)	—
2	Input to PC 1	8,400	~400 (est.)	—
3	Input to PC 2	4,400	200	—
4	After Air Spatial Filter Pinhole	1,800	80	—
5	At HO 2 Input	1,250	40 - 50	0.0044
6	At HO 3 Input	550	20 - 30	0.08 - 0.10
7	At HO 4 Input	480	~20	1.88
8	Driver Output	330	~15	16.40

G1056

Table 1
OMEGA driver baseline energy at maximum output with 1 nsec oscillator pulses (November, 1981).

The distribution of OMEGA system shots during this period was as follows:

Target Shots	38
OMEGA Test Shots	78
Driver Line Test Shots	117
Software Test Shots	131
TOTAL	364

1.C Photoacoustic Absorption Spectroscopy for Defect Analysis in Thin Films

Laser-induced damage to optical thin film coatings is the fundamental limitation in the design and construction of large laser systems used to investigate the feasibility of energy generation through thermonuclear fusion. Recent work by several groups has suggested that this damage is caused by the presence of defects on the order of one micron in dimension located in the thin film or at the film-substrate interface.[1,2] Impurities are one type of defect, but another type might be non-stoichiometric regions of the coating. In an attempt to establish more clearly the existence of these defects, and their relationship to laser-induced damage, we have begun to examine numerous optical micro-analytical techniques. In this article we discuss the use of photo-acoustic absorption spectroscopy (PAS) to locate absorbing defects in dielectric thin films.

In PAS a laser beam is focussed onto a thin film-coated substrate contained within a specially designed cell. The portion of the coating being irradiated will heat if it contains an impurity that absorbs at the laser

wavelength. The air confined to the cell and adjacent to the coating will also experience a temperature rise as heat flows to it from the impurity. By mechanically chopping the laser beam a periodic pressure wave is produced which can be detected by a microphone built into the photoacoustic absorption cell. The magnitude of the acoustic signal detected correlates well with the absorption strength of the impurities in the coating.

PAS offers a versatility not found in other techniques like laser calorimetry. With highly sensitive microphones, phase-locked electronic processing technology, and tightly focussed laser beams, PAS is capable of detecting absorbing sites a few microns in diameter possessing absorption coefficients of $10^{-4}cm^{-1}$. By scanning the laser across the coated part or moving the part under the focussed beam, a two-dimensional map showing the sizes and locations (clustering) of impurities can be generated. By varying the laser wavelength, a photoacoustic spectrum that faithfully replicates an optical absorption spectrum can be obtained that might ultimately make impurity identification possible. The single most severe limitation to the use of PAS is its sensitivity to acoustic noise. Care must be taken to locate PAS experiments in a relatively noise-free environment, and to employ laboratory equipment (lasers, mechanical choppers, stepper motors) that generate little acoustic noise.

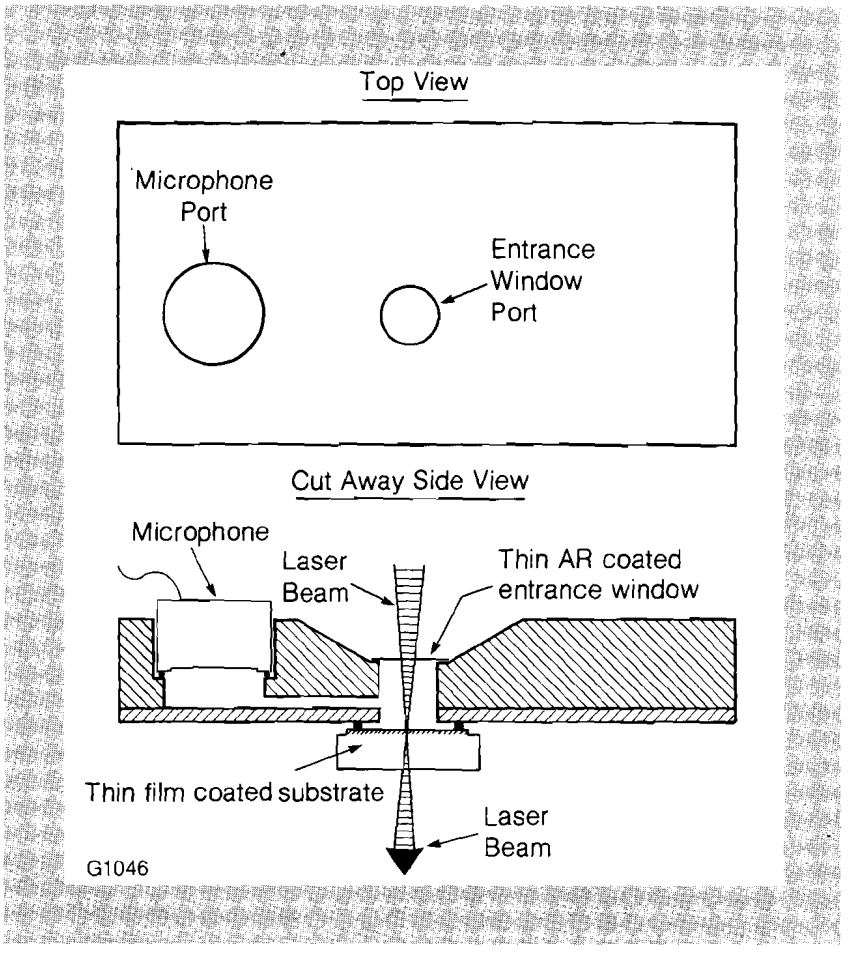

Fig. 2
Design of photoacoustic absorption cell. The distance between the entrance window and coated substrate surface (2mm), and the diameter of the narrow passage between the sample air chamber and the microphone air chamber (1.5mm) are minimized to enhance the signal-to-noise ratio of the cell. The microphone is a Buel and Kjaer model 4144 (25mm diameter) with a 100 Å thick diaphragm.

Experiments using PAS at Rochester started in the late 1970's with lasers operating in the infrared at wavelengths of 10,600 nm and 1060 nm and with focal spot sizes between 100 and 200 microns in diameter.[3,4] Work described here uses a Coherent Radiation CR6 argon ion laser operating at any one of several selectable wavelengths in the visible between 514.5 nm and 476.5 nm, a focussed spot size 6 to 8 microns in diameter, and a photoacoustic cell modified from a previous in-house design.[4] A schematic representation (not to scale) of the cell design is given in Fig. 2. A key to minimizing the cell's sensitivity to background acoustic noise is the reduced size of the air chambers above the sample, below the microphone and in the connecting passageway. Measurements on uniformly absorbing samples demonstrate that a laser-chopping frequency of 355 Hz gives the optimum signal-to-noise performance for this modified cell.

A block diagram of the components that comprise the photoacoustic absorption apparatus is given in Fig. 3. X-Y translation stages with stepping motors driven by commands from a minicomputer control the movement of the stage supporting the cell. Acoustic signals are preamplified and sensed by a lock-in amplifier referenced to the 355 Hz mechanically chopped frequency of the incident laser beam. The minicomputer stores lock-in amplifier data on floppy disks for off-line reprocessing, and also generates hard copy two-dimensional maps on a strip chart recorder. An attractive feature of the translation stages is that their absolute locations are displayed digitally on each controller. This provides an origin to which any scan may be referenced.

Fig. 3
Block diagram of photoacoustic absorption apparatus. A Southwest Technical Products Corporation 6800 minicomputer with a Motorola 6800 microprocessor controls acquisition and storage of acoustic signals from a Princeton Applied Research model 124 lock-in amplifier. The computer also operates the translation stages, manufactured by Aerotech, Inc., to scan in raster fashion the coated parts beneath the laser beam.

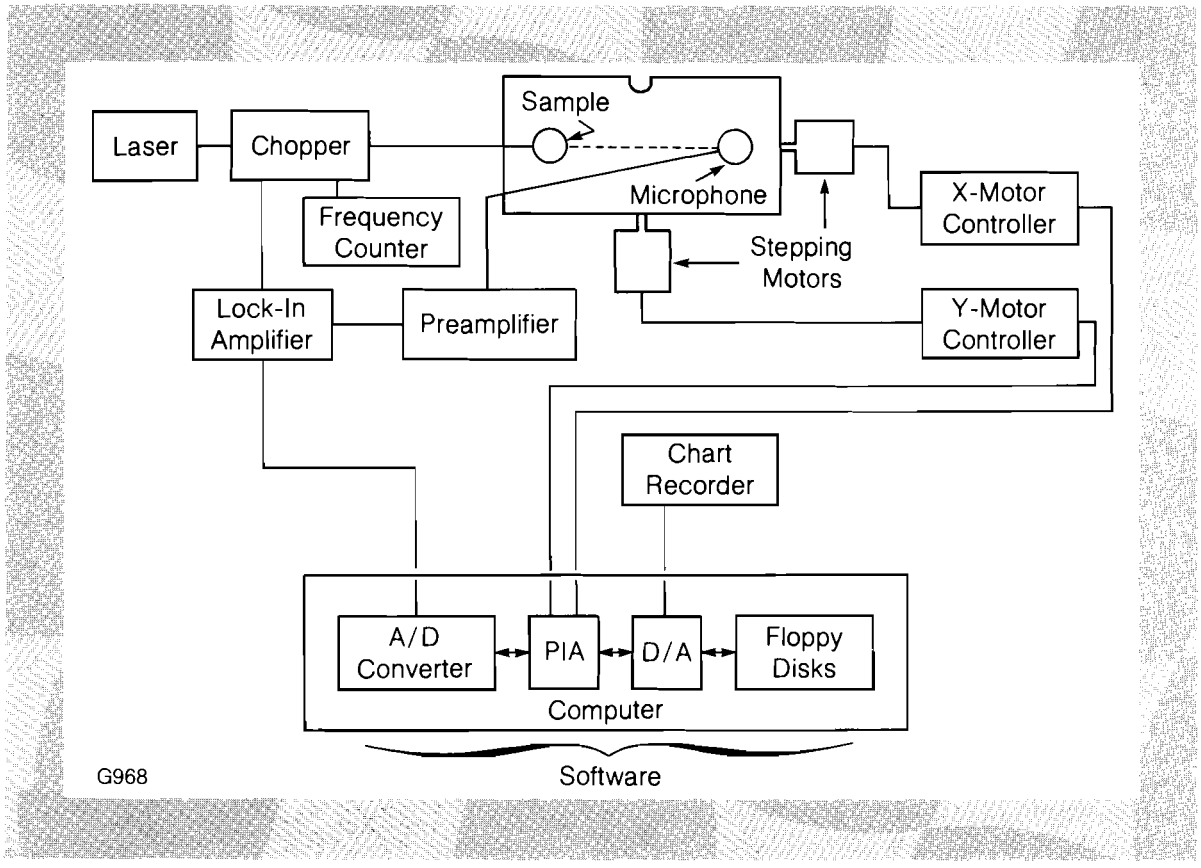

The ultimate resolution and sensitivity of this apparatus are demonstrated by the data shown in Fig. 4. By working with polystyrene balls from fifteen microns to one micron in diameter the minimum detectable ball size using a focussed laser beam eight microns in diameter was determined to be two microns. The photoacoustic signal generated by this barely resolvable ball corresponds to an absorption coefficient of $5 \times 10^{-4} cm^{-1}$.

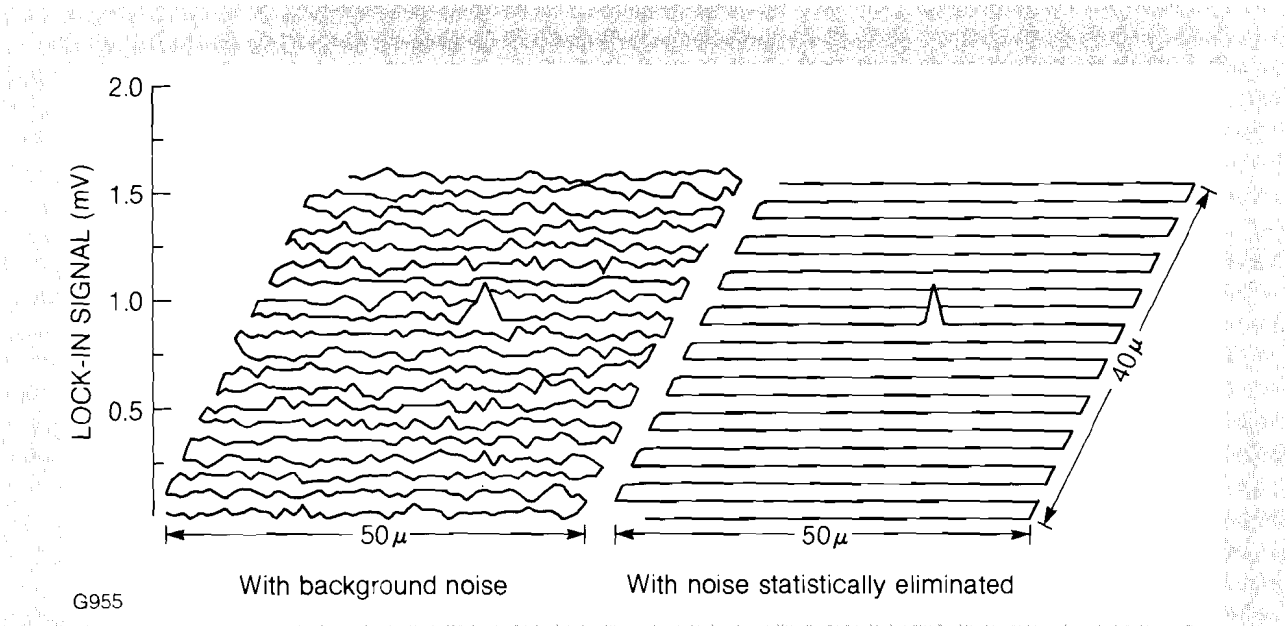

Fig. 4
Photoacoustic signals generated from a raster scan of a 2 micron diameter polystyrene ball on a bare glass surface. Computer-aided statistical analysis of stored data to eliminate background noise indicates that the apparatus can detect absorbing sites 2 microns in size. This scan was generated with the argon ion laser operating at a wavelength of 0.5145 microns with an output power of 150mW.

The spectral response of the photoacoustic absorption apparatus has been examined in two ways. Figure 5 shows the acoustic signal obtained from carbon black powder on a glass substrate support as a function of laser wavelength from 476.5 nm to 514.4 nm. Carbon black exhibits its wavelength-independent absorption in the bluegreen spectral

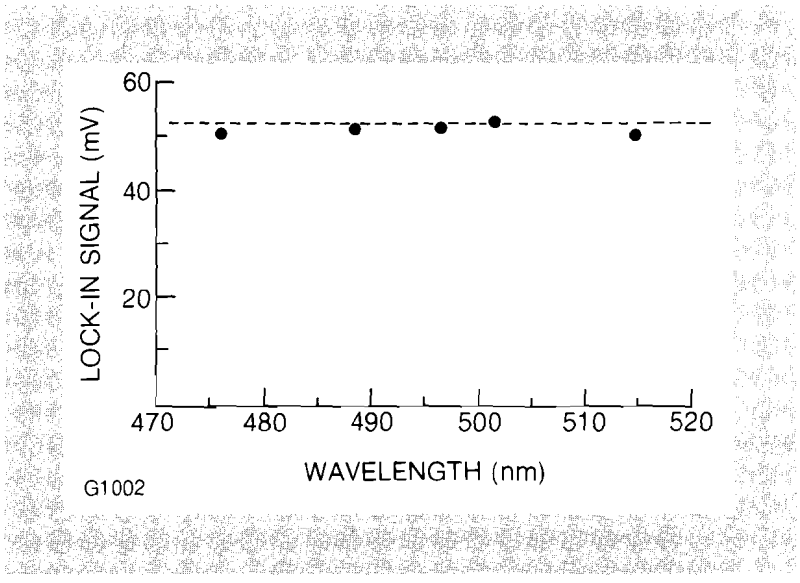

Fig. 5
Photoacoustic signal from carbon black. The response is in agreement with optical absorption data which shows carbon black to be a uniformly flat absorber in the bluegreen region of the spectrum.

region,[6] and this is confirmed by the photoacoustic response. Figure 6 gives the acoustic signal from a sample of neodymium-doped glass that has been examined over the same wavelength range. The wavelength-dependent optical absorption signature of the Nd^{+3} ions, as generated from spectrometer scans, is faithfully replicated by the photoacoustic signal.

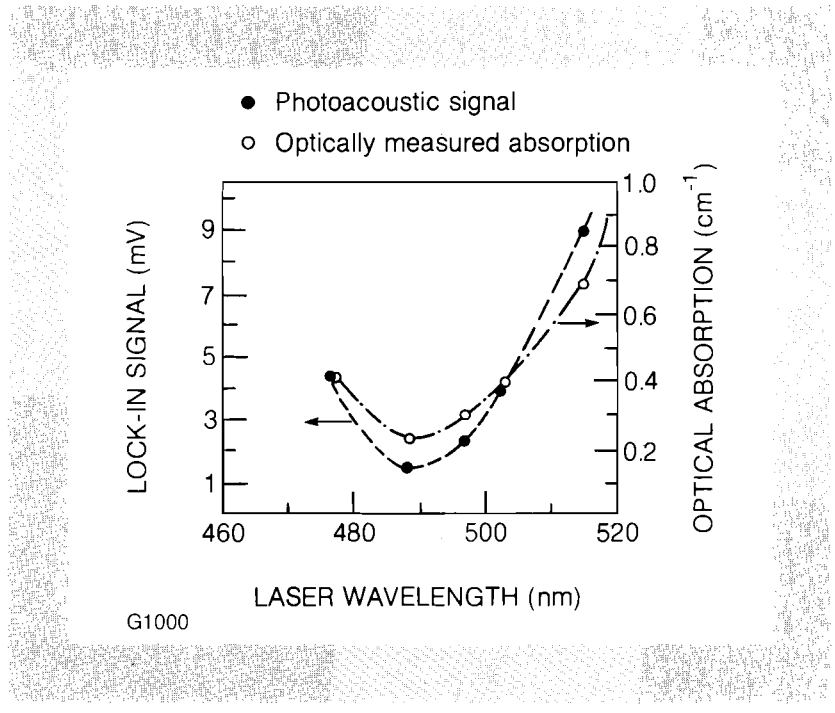

Fig. 6
Photoacoustic absorption signal compared to optical absorption for sample of neodymium-doped glass. The wavelength dispersion of optical absorption exhibited by the Nd^{+3} ions is reproduced by the photoacoustic absorption signature after adjusting the acoustic signal scale so that the optical and acoustic data points coincide at a wavelength of 476.5 nm.

We have begun to utilize the photoacoustic absorption apparatus for the analysis of defects in dielectric thin film coatings composed of multiple alternating layers of high refractive index and low refractive index metal oxides. Such coatings are commonly employed to impart antireflecting, partly reflecting, or highly reflecting properties to the surfaces of lenses, windows, beamsplitters, and mirrors used in LLE's OMEGA laser system. Spatter is a type of defect sometimes found in these coatings, which occurs when materials being evaporated onto a substrate are instead ejected from the source as small, unevaporated particles. Oxidation of evaporants during coating deposition and post-deposition baking is required to impart appropriate mechanical and optical properties to a multilayer coating. Spatter sites represent portions of a coating that are prevented from achieving proper stoichiometry and structure because they are significantly less reactive than evaporated material in an oxygen atmosphere. Because of their altered composition, spatter sites can exhibit optical absorption which is larger than that of the surrounding stoichiometric coating material.[7]

Nomarski microscopy was used to locate titanium dioxide spatter sites that were intentionally generated in a TiO_2/SiO_2 multilayer coating on a BK-7 substrate by the Optical Coating Facility of the Institute of Optics. Scanning photoacoustic absorption spectroscopy was subsequently performed over a 50 micron by 40 micron region of the coating that contained one TiO_2 site 10 microns in diameter. PAS scans taken at

five laser wavelengths are shown in Fig. 7. The anomalously large absorption of this spatter site compared to the coated background is apparent. An inspection of the figure also shows that the absorption at this site increases as the laser wavelength decreases from the green to the

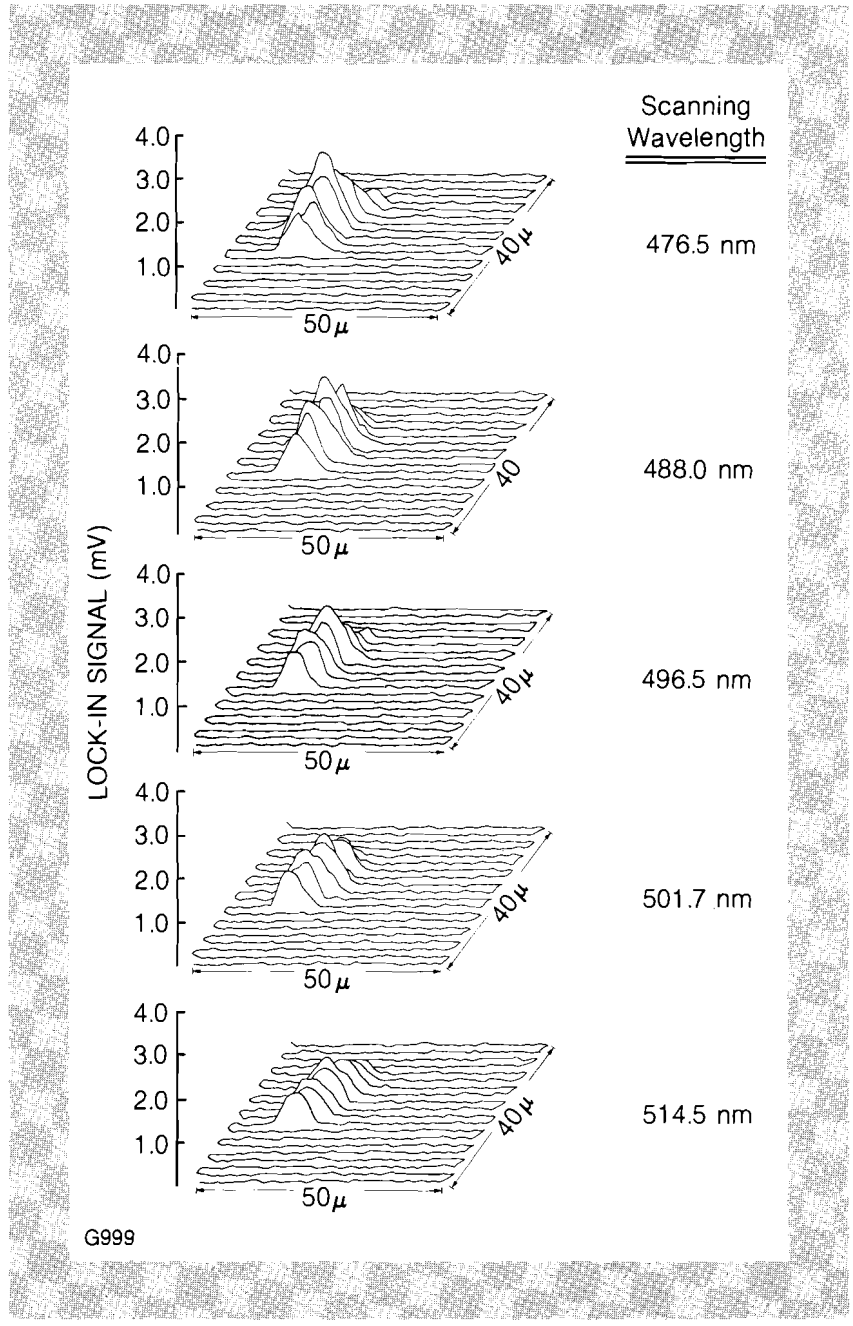

Fig. 7
Scanning photoacoustic absorption spectroscopy of a TiO_2 spatter site embedded in a TiO_2/SiO_2 multilayer dielectric thin film coating. The laser intensity at each wavelength was kept constant at a level of 145mW.

blue. By plotting the peak photoacoustic signal detected in each scan versus wavelength, the dispersion curve in Fig. 8 is obtained. From this curve it is evident that the wing of the ultraviolet absorption edge for the material in this spatter site begins at a wavelength near 500 nm. Optical spectrophotometry on a single 700 Å thick stoichiometric layer of TiO_2 indicates, however, that this wing should not be apparent until a wavelength of 350 to 400 nm. It is clear from this example that PAS offers an

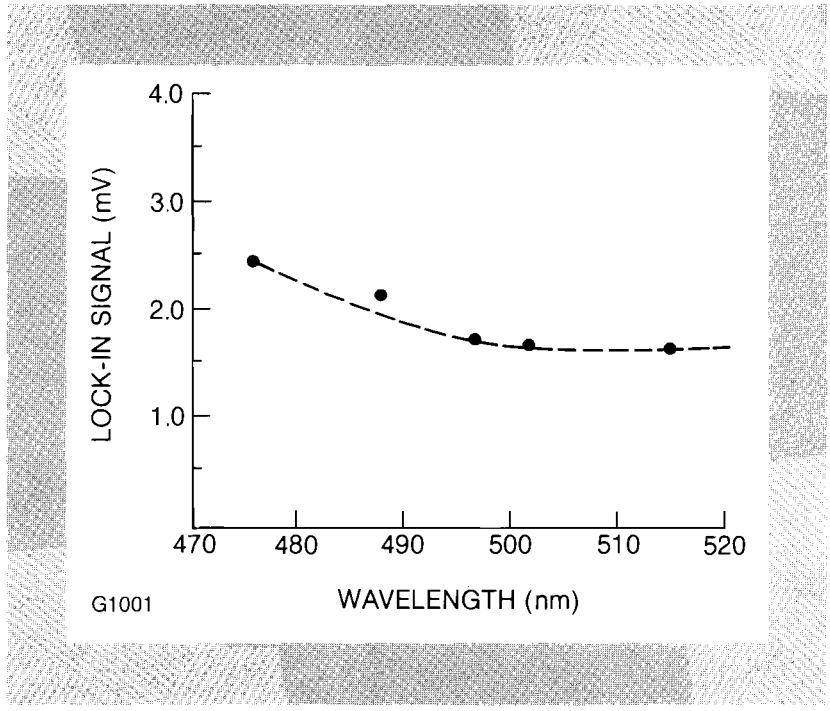

Fig. 8
Wavelength dispersion of the absorption in the TiO_2 spatter site as measured by plotting the maximum photoacoustic signal from each wavelength scan in Fig. 7. The increase in absorption observed to begin here at a wavelength of 500 nm commences in TiO_2 of proper stoichiometry at a lower wavelength near 350 nm to 400 nm.

excellent means for non-destructively probing small defects in dielectric thin films to elicit their absorptive behavior.

Photoacoustic absorption spectroscopy in conjunction with other optical microanalytical techniques should, in future work, contribute to our understanding of defects in multilayer dielectric thin films. The characterization of defect properties such as optical absorption can lead to their identification, and a modification in coating deposition procedures to reduce defect number densities will ultimately increase the laser-damage resistance of coated laser system components.

REFERENCES

1. T. A. Wiggins, T. W. Walker and A.H. Guenther, *NBS Special Publication 620: Laser-Induced Damage in Optical Materials*, 277-286 (1980).
2. W. H. Lowdermilk and D. Milam, *IEEE J. Quantum Electron.* **QE17**, 1888 (1981).
3. R. P. Freese and K. Teegarden, *NBS Special Publication 568: Laser-Induced Damage in Optical Materials*, 313-332 (1979).
4. R. D. Jacobs, MS Thesis, Institute of Optics, University of Rochester (1979).
5. D. S. Atlas, MS Thesis, Institute of Optics, University of Rochester (1981).
6. J. Ravey and S. Premilat, *J. Chim. Phys.* **6-7**, 1913-1921 (1970).
7. W. Heitman, *Appl. Opt.* **10** (11) (November 1971).